

International Conference on Space Optics—ICSO 2018

Chania, Greece

9–12 October 2018

Edited by Zoran Sodnik, Nikos Karafolas, and Bruno Cugny



Integration ghosts in interferograms: origin and correction

D. Lamarre

C. Keim

T. Guggenmoser



icso proceedings



Integration Ghosts in Interferograms: Origin and Correction

D. Lamarre^{1a}, C. Keim^b, and T. Guggenmoser^a

^aEuropean Space Agency, Keplerlaan 1, 2201 AZ Noordwijk, The Netherlands.

^bAirbus DS GmbH, 81663 München, Germany.

ABSTRACT

We report on an error source and a possible correction which occurs with Fourier Transform Spectrometers due to the use of an integrating detector.

The new class of imaging Fourier-Transform-Spectrometers (FTS) is in many cases best realised using continuously moving mirrors and an integrating array detector with fixed frame rate. In case of not perfectly constant optical path difference (OPD) speed, this corresponds to an irregular OPD sampling, resulting in radiometric errors. This effect is well-known and can be solved by resampling, i.e. interpolation on a regular OPD grid.

A less known effect is caused by the detector integrating over constant time intervals, which – like the sampling steps - are also of varying length in the OPD domain due to the non-constant OPD speed. The resulting error is discussed in the presented paper, where also an elegant correction method is proposed.

Constant-width integration in the OPD domain acts as a spatial low-pass filter on the interferogram. If the integration width varies, a modulation is applied to the interferogram's envelope. This modulation results in a radiometric error in the spectrum.

The presented correction is a finite impulse response filter with only three taps, to be applied to the measured time-sampled interferogram before resampling. In case the interpolation is done with filters, these filters and the new 3-tap filter can be combined to reduce processing overhead.

Keywords: Fourier Transform Spectrometer, integrating detector, equi-time sampling, modulation efficiency, spectral ghosts, correction.

1 INTRODUCTION

A Fourier transform spectrometer (FTS) splits the incoming light into two beams, which travel separate paths. At the detector, the two beams, which now have a phase difference, are brought to interference. Therefore the intensity of the detected signal depends on the optical path difference (OPD) of the two light paths. To measure a so-called interferogram, the OPD is varied and the signal is recorded as function of the OPD. Mathematically, the interferogram is the Fourier Transform of the incident spectral radiance. Therefore, the incident spectrum can be reconstructed by a Discrete Fourier Transform of the measured interferogram, sampled at discrete OPD positions. To speed up the Fourier Transform over several thousand points an FFT is a good choice. This implies that the sampling positions are on a regular grid, i.e. equidistant in OPD.

A moving mirror (which can be a retroreflector) is often used in one or both paths. The OPD is measured with a laser, traveling the same paths as the light and equally creating an interferogram. The laser interferogram is a cosine wave, which is maximum for any OPD position corresponding to an integer multiple of the laser wavelength. Classically, the interferogram is sampled where the laser interferogram is zero; this ensures the regular OPD grid.

While care had to be taken in the design of amplifiers to adequately take into account time delays between interferogram acquisition and laser reference signal, little post processing was further required for concerning sampling. This design is still widely used.

However, there is an increasing interest for an equi-time sampling as proposed by Brault¹, in particular for imaging spectrometers. For the equi-spatial sampling, either the delay must be perfectly compensated for (impossible when the delay is frequency dependent) or the OPD speed must be perfectly constant, to avoid radiometric errors due to sampling errors. For the equi-time sampling these needs are relaxed, as we only need to know perfectly the delay (and its frequency dependency) and the OPD speed. While relaxing the mechanical requirement Brault's equi-time sampling approach also simplifies the detector operation, especially of integrating array detectors. Further, with the read out at constant frame rate, the integration time can be maximized to sense as much as possible of the available signal.

For the equi-time sampled interferogram, basically two different types of error are caused by OPD speed variation:

¹daniel.lamarre@esa.int, corneli.keim@airbus.com, tobias.guggenmoser@esa.int

- a) the sampling is irregular in the opd domain. As found by Brault, this error can be compensated for by an interpolation on a regular opd grid. The interpolation can consider detection chain and reference signal delays and also allows to sample on the centres of the integration intervals. As Brault's algorithm and its implementation is wide spread and in detail discussed elsewhere, it will not be further described here and its application is assumed for the remainder of this paper.
- b) The integration window is not constant in the opd domain. At high interferometer speed, a fixed duration integration window covers a larger width in OPD space than at low speed. The variation of the integration window causes an amplitude modulation of the interferogram. The radiometric error resulting from these amplitude ghosts can be attenuated by the new correction method, described in the body of this paper.

The paper is organised in two parts. In the next paragraph, the mathematical description of the error source and its correction is developed. In the final paragraph, we give examples of the correction capability.

2 MATHEMATICAL DESCRIPTION OF GHOSTS AND THEIR CORRECTION

2.1 Origin of integration ghosts

2.1.1 Modulation efficiency

We first assess the impact of an integration of the interferogram in the opd domain. The integration can be understood as a convolution with a boxcar.

$IFG(x) = ifg(x) * rect(\Delta x)$	x: OPD position ifg(x): the interferogram IFG(x): the integrated interferogram Δx : the integration window rect(Δx): the boxcar of width Δx *: the convolution operator	(1)
------------------------------------	--	-----

Transition to the spectral domain gives a multiplication of the original spectrum with the Fourier transform of the boxcar, which is a sinc function.

$S(\sigma) = s(\sigma) \cdot sinc(\pi \cdot \Delta x \cdot \sigma)$	σ : the spectral position s(σ): the spectrum S(σ): the spectrum of the integrated interferogram	(2)
---	--	-----

The integration in the OPD domain scales the raw spectral signal. The scaling depends on the wavenumber, and also on the integration window length. The scaling does not directly cause a radiometric error, as the sinc factor cancels when the same integration window length is chosen in the calibration interferogram.

The term $M = sinc(\pi \cdot \Delta x \cdot \sigma)$ is called modulation efficiency. We understand the naming, when looking at a monochromatic interferogram, which is a cosine function. The amplitude of the cosine reflects the usable signal strength. The integration over the window effectively reduces the amplitude of the cosine.

2.1.2 Integration over constant time windows

We now look what happen for a real system where the integration is done in the temporal domain. For perfectly constant OPD speed, the integration is equally done over constant OPD windows. For a varying OPD speed, the OPD windows scale with the OPD speed:

$\Delta x(t) = \Delta t \cdot v(t)$	Δx : the integration window in the OPD domain Δt : the (constant) temporal integration window v(t): the OPD speed, which is a function of time	(3)
-------------------------------------	--	-----

As the window in Eq (3) is not constant, it cannot replace the convolution kernel in Eq(1). To do so, we must explicitly write the integral form:

$IFG(x) = \int_{x-0.5\Delta t \cdot v(x)}^{x+0.5\Delta t \cdot v(x)} ifg(x') dx'$	(4)
---	-----

As Eq(4) is not a convolution in the mathematical sense, the derivation of the spectrum is not as easy, as in Eq(2). We ignore this fact, and develop the spectrum for the special case of a monochromatic input scene with a harmonically perturbed OPD speed.

We write the harmonically varying OPD speed as:

$v(t) = (1 + a \cdot \sin(\omega t + \varphi)) \cdot v_0$	v_0 : the nominal OPD speed a : the amplitude of the OPD speed variation ω : the frequency of the OPD speed variation φ : a phase term, determining the speed at $t=0$ (ZOPD)
---	---

We further give the (normalised) interferogram of a monochromatic source (wavenumber σ_0) as:

$ifg(x) = (1 + \cos(2\pi\sigma_0 x))$	x : the OPD σ_0 : the wavenumber
---------------------------------------	--

The resulting interferogram, after integration is shown in black in Fig. 1, compared to the same interferogram integrated over constant OPD-windows (the averaged one) in magenta. In order to compute the interferogram (4), we convolve over the ordinary, unperturbed averaging window, factoring out the OPD-dependence into a scaling function $K(x)$. After some transformation and a first order Taylor development we get a good estimation of K .

$IFG(x) = ifg(x) * rect(\Delta t \cdot v(t))$ $\approx (ifg(x) * rect(\Delta t \cdot v_0)) \cdot K(x)$ $K(x) \approx 1 + (v(t(x)) - v_0) \cdot \frac{dsinc(\pi \cdot \Delta t \cdot v \cdot \sigma_0)}{dv} \Big _{v=v_0}$ $\approx 1 + (v(t(x)) - v_0) \cdot b$ $\approx 1 + v_0 a \cdot \sin(\omega t + \varphi) \cdot b$	$K(x)$: the resulting interferogram scaling term (7) $b=b(\Delta t, v_0, \sigma_0)$: The slope of the modulation efficiency, acting as amplitude of the harmonic interferogram modulation
--	--

We can now do the Fourier transform of IFG(x).

$S(\sigma) \approx (s(\sigma) \cdot sinc(\pi \cdot \Delta x \cdot \sigma)) * k(\sigma)$	σ : the spectral position (8) $s(\sigma)$: the unaffected spectrum $S(\sigma)$: the spectrum after integration Δx : the averaged OPD integration window (for $v=v_0$) $k(\sigma)$: the FT of $K(x)$
---	--

With the setting of $x=v_0 \cdot t$ in the sine term of the OPD variation, we analytically can give the FT of $K(x)$. The induced error is of second order, and it is easily shown that the ignored ghosts have much smaller amplitude than the two considered ones. With the given approximations, the ghosts due to a harmonic OPD speed variation become classical amplitude ghosts.

$k(\sigma) \approx \delta(\sigma - \sigma_0)$ $-i \cdot e^{i\varphi} \cdot \frac{ab}{4} v_0 \cdot \delta(\sigma - \sigma_0 - \Delta\sigma)$ $+i \cdot e^{-i\varphi} \cdot \frac{ab}{4} v_0 \cdot \delta(\sigma - \sigma_0 + \Delta\sigma)$	σ : the spectral position (9) σ_0 : the monochromatic wavenumber φ : the phase of the OPD variation, at ZOPD $\Delta\sigma = \frac{\omega}{2\pi v_0}$: the distance of the ghosts $k(\sigma)$: the FT of $K(x)$
--	---

We realise from Eq(9) that the ghosts' amplitude depends on the amplitude of the OPD variation a , but also on b , the sensitivity of the modulation efficiency wrt. speed variation. This briefly brings us to the correction idea; we simply make b close to zero. How this can be done will be described in detail later in this paper.

Fig. 1 compares the monochromatic interferograms, resulting from integration over constant opd-windows (magenta curve) and from integration over constant time-windows (black curve) for harmonic OPD speed variations. Fig. 2 shows the corresponding spectra with the ghosts left and right of the original line.

The monochromatic interferogram could be easily corrected by dividing the interferogram value by the modulation efficiency. All we need to know is the OPD speed at the interferogram sampling positions. This information is needed for the resampling anyway.

The continuous spectrum can be decomposed into monochromatic lines:

$IFG(x) = \int_0^\infty ifg_\sigma(x) \cdot sinc(\pi \cdot \Delta x(x) \cdot \sigma) d\sigma$	(10)
---	------

The difficulty of the correction for the continuous spectrum is that the modulation efficiency depends on the wavenumber. We can calculate the scaling of the interferogram at every sampling point by summing all wavenumbers over the monochromatic interferogram and the (monochromatic) modulation efficiency at that point. To set up a correction, we can use an iterative process, where the measured spectrum is used to get the first interferogram scaling. The first corrected spectrum is transformed from the measured interferogram divided by the first interferogram scaling. This spectrum can be used again to get the second interferogram scaling, and so on. This correction works, but is very costly in terms of processing.

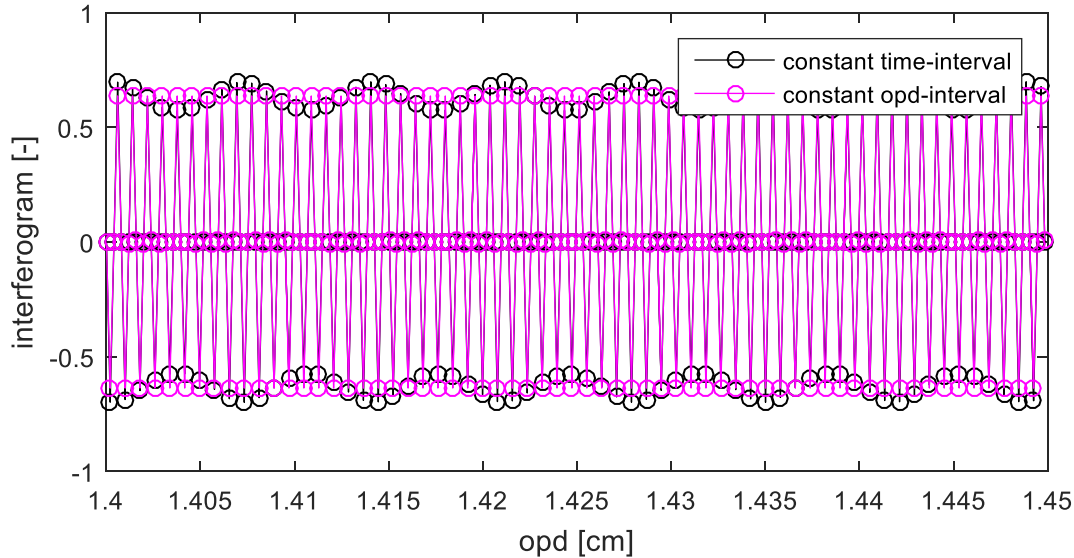


Fig. 1 The figure compares the interferogram resulting from integration over constant time windows (magenta) with that after integration over constant OPD-windows (black). The interferogram sampling is on an equi-spatial grid in both cases. The parameters of the spectrum, the sampling, and the exaggerated perturbation have been chosen to be well distinguishable in the plot.

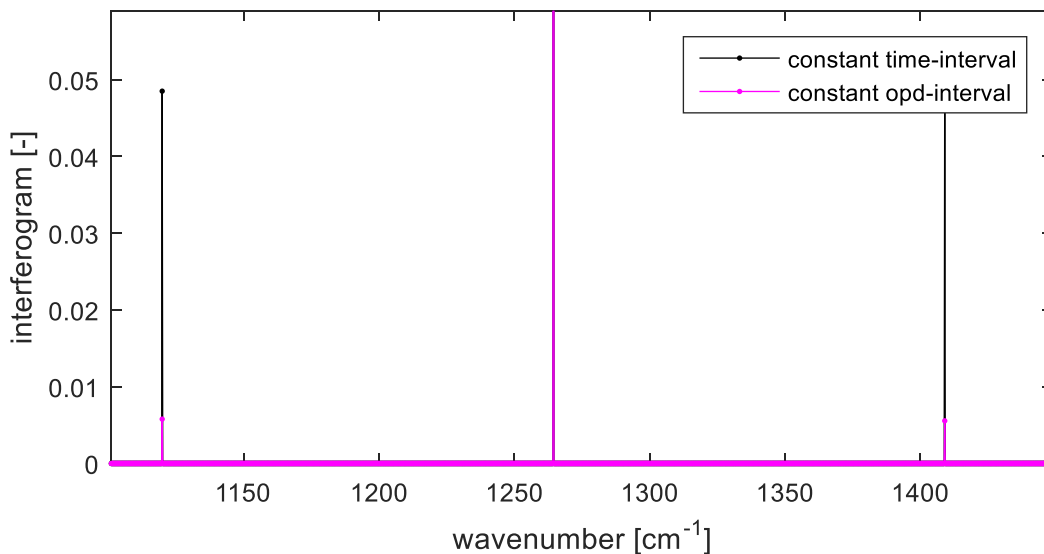


Fig. 2 The figure shows the Fourier transformation of the interferograms in Fig. 1. The spectra are normalized such that the magnitude of the original line in the centre, i.e. at 1260cm^{-1} , is one.

2.2 Correction of the Ghosts

We have seen in the last paragraph that the root cause of the ghosts is the variation of the modulation efficiency with OPD speed. In the monochromatic case, the size of the ghosts is proportional to the slope b of the modulation efficiency. Let us assess what happens when the interferogram is additionally multiplied with a second function $g(v)$. The amplitude of the interferogram is then altered depending on the linearization of the product $M \cdot g$, and the ghosts magnitude is proportional to the slope $d(M \cdot g)/dv$. This means, if we find a function g such that the slope of the product is zero, then the ghosts vanish. The proposed novel correction is basically such a function g .

2.2.1 The correction method

The method consists in performing a convolution of the equi-time sampled interferogram with a special 3-tap filter. This convolution is applied before the resampling on the equal OPD grid. The filter is of the type:

$$g(k) = q \cdot \left[\frac{k}{2} \quad 1 - k \quad \frac{k}{2} \right] \quad (11)$$

Because the filter is symmetrical, it does not cause phase changes, i.e. it does not affect the positions of the samples. For the special choice of $q=1$ the sum of the elements is unity, thus the filter is neural at zero frequency.

We get the function $g(v)$ by Fourier transformation of the filter. The Fourier transformation can be more easily seen, for the filter separated into its two basic components:

$$g(k) = q \cdot \left[\frac{k}{2} \quad 0 \quad \frac{k}{2} \right] + q \cdot [0 \quad 1 - k \quad 0] \quad (12)$$

The first filter term is symmetrical and with single frequency (only one tap on each side of the centre tap), and is then represented in the Fourier domain as a cosine. The period of this cosine is the inverse of the sampling period. The second filter term only multiplies the input signal by a constant.

$ifg_c(t) = ifg(t) * g(k)$ $ifg_c(x) = resampling(ifg_c(t))$ $S_c(\sigma) = S(\sigma) \cdot q \cdot [k \cos(2\pi v T \sigma) + (1 - k)]$	T : Integration time (s) (13) $ifg_c(t)$: Interferogramme obtained after convolution $S_c(\sigma)$: Spectrum, or Fourier transform, of $ifg_c(x)$
--	---

The first filter term must be chosen so as to compensate the slope of the modulation efficiency, i.e. so that the slope of $M \cdot g$ is zero. This defines the value of $q \cdot k$. The second filter term has no impact on the ghosts and can be chosen for convenience. Either choice of it must be identically chosen in the calibration spectrum, so that the scaling with a constant cancels during radiometric calibration. In case the interferogram amplitude does not matter, the simple choices of $q=1$ or $q(1 - k) = 1$ are rather convenient. Another sensible setting is $q(1 - k) = 1 - qk \cdot \cos(2\pi v_0 T \sigma_0)$. The latter results in $\langle g \rangle = 1$, therefore the energy of the interferogram is not changed by the convolution. Therefore this setting was chosen in all presented figures. Fig. 3 shows the modulation efficiency (blue) together with the Fourier transform of the correction filter (magenta) for a speed variation of 10%. The black curve in the same figure shows that the filter works and the slope of the product of the functions is zero for the mean OPD speed, and the central wavenumber. Fig. 4 shows the equi-time sampled interferogram (\cdot) and interferograms (\circ) resampled on an equi-spatial grid with and without preceding filter. The filter is switched off by setting $k=0$. Comparing the resampled interferograms in this figure with the interferograms in Fig. 1 illustrates how the filter works. Without the filter, the resampled interferogram is similar to an interferogram sampled on the correct positions but with constant integration time windows, while the resampling with preceding filter leads to an interferogram similar to that sampled at the correct OPD positions and integrated over constant OPD windows.

In the monochromatic case, the selection of $q \cdot k$ is straightforward. The situation changes for a broad band spectrum. Generally, a first guess can be derived for the central wavenumber, already keeping the variation of $M \cdot g$ small over the range $[\min(v) \cdot \sigma_{\min}, \max(v) \cdot \sigma_{\max}]$. Dependent on a given set of requirements, the parameter can be further fine-tuned, e.g. to minimize the radiometric error for an applicable reference scene.

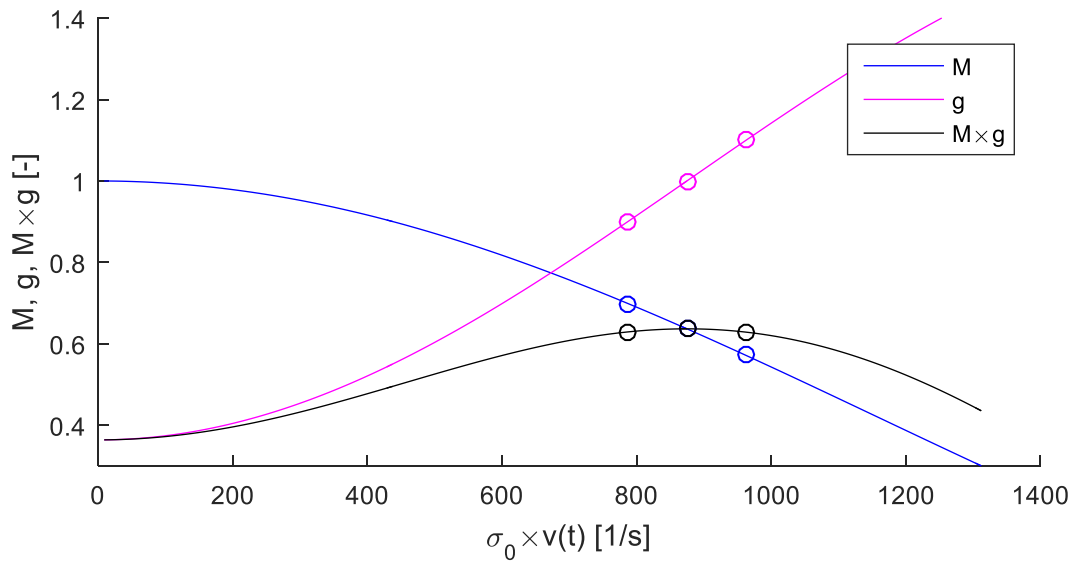


Fig. 3 The modulation efficiency M , the correction function g , and their product are shown for one wavenumber $\sigma_0=1264\text{cm}^{-1}$ and an OPD speed in the range 0 to 1cm/s. The circles indicate the velocity range $\pm 10\%$ around the nominal OPD speed $\bar{v} = 0.69\text{cm/s}$, for which the correction filter is optimized.

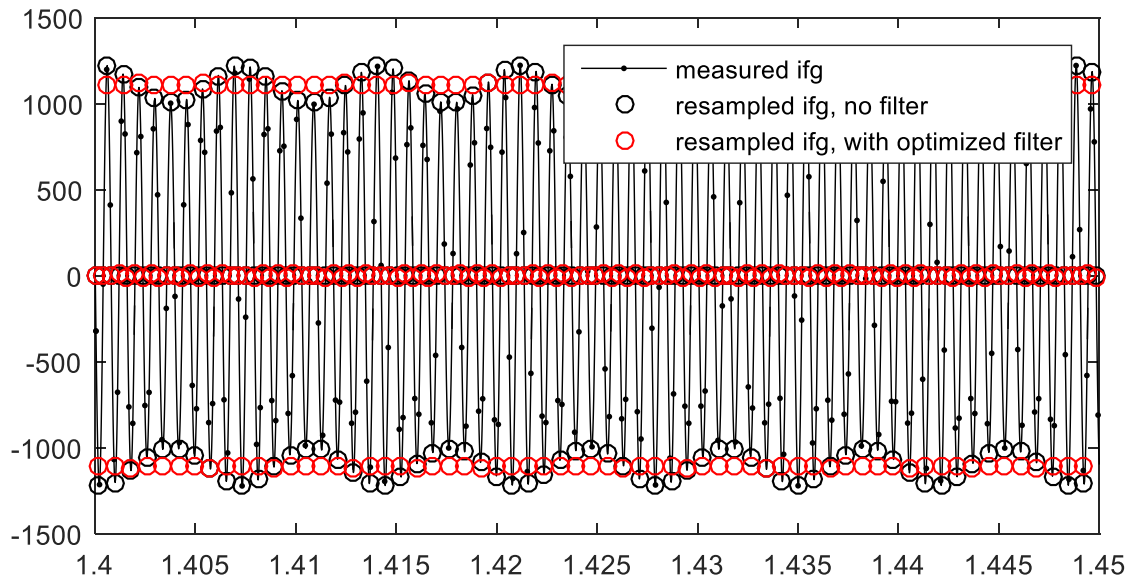


Fig. 4 The solid line is the measured, equi-temporal sampled ifg, with the dots giving the position of the sampling. The circles give the resampled ifg, with and without ($k=0$) preceding filter.

3 THE CAPABILITY OF THE FILTER IN CASE OF PREMIER

3.1 The Earth-explorer candidate Premier

Premier² is an imaging FTS operating in rearward limb geometry. It is measuring in the thermal infrared spectral range. Premier was proposed as candidate for the 7th Earth-explorer mission, but down selected in 2013. For the assessment presented in this proceeding, it was chosen do to its clear radiometric requirement on spectral ghosts.

3.2 Radiometric requirement

The dedicated requirement on ghosts limits there radiometric impact, which is considered as noise due to the random phase of the ghosts. The requirement is cited below:

ILS-570

The radiometric errors resulting from SRF perturbations generated by modulation shall be smaller than $1.5 \text{ nW}/(\text{cm}^2 \text{ sr cm}^{-1})$ in atmospheric dynamics mode and smaller than $4 \text{ nW}/(\text{cm}^2 \text{ sr cm}^{-1})$ in atmospheric chemistry mode.

The requirement is applicable over Premier's dynamic range; hence it is driven by the maximum signal. The radiometric error due to ghosts was therefore evaluated for 240K Black-body radiance, which is the upper limit of Premier's dynamic range.

3.3 The residual radiometric error due to corrected integration ghosts

For Premier, the sampling frequency was traded-off between 2467Hz and 4000Hz. Therefore, for both frequencies the radiometric error due to integration ghosts has been simulated with and without the correction filter. As expected from the equations in § 2 the ghosts are smaller for a faster sampling. Also with the correction, the residual error is smaller for the faster sampling.

Premier was planned to acquire interferograms in two modes: the 'chemistry' mode with a larger MOPD and faster OPD speed but longer dwell time, leading to finer spectral resolution but coarser spatial sampling and the 'dynamics' mode with shorter dwell time due to shorter MOPD and slower OPD speed which leads to a finer spatial sampling but coarser spectral resolution. As we can conclude from the equations, the slower OPD speed creates smaller ghosts, which is again still the case including the correction.

From the exhaustive analysis we present the results for the most interesting case, which is 'chemistry'-mode in 2467Hz

Premier split the wide spectral range with a large radiometric dynamics into two bands to limit the photo-noise cross talk. These are band A [710 cm⁻¹ to 1010 cm⁻¹] and band B [1070 cm⁻¹ to 1650 cm⁻¹]. We present the ghosts and the correction efficiency for both bands in several disturbance cases in Fig. 5 through Fig. 8. The measure for the radiometric error is according to the requirement.

4 CONCLUSION

We have shown that the radiometric error due to integration ghosts can be effectively reduced with a simple filter. The application of the filter is neutral wrt processing, as it can be included into the interpolation filter.

5 REFERENCES

- [1] Brault, J. W., "New approach to high-precision Fourier transform spectrometer design", Appl. Optics, 35, 2891–2896, (1996).
- [2] ESA, "Report for Mission Selection: PREMIER", ESA SP-1324/3, May 2012, <<https://earth.esa.int/web/guest/document-library/browse-document-library/-/article/premier-report-for-mission-selection-an-earth-explorer-to-observe-atmospheric-composition>>

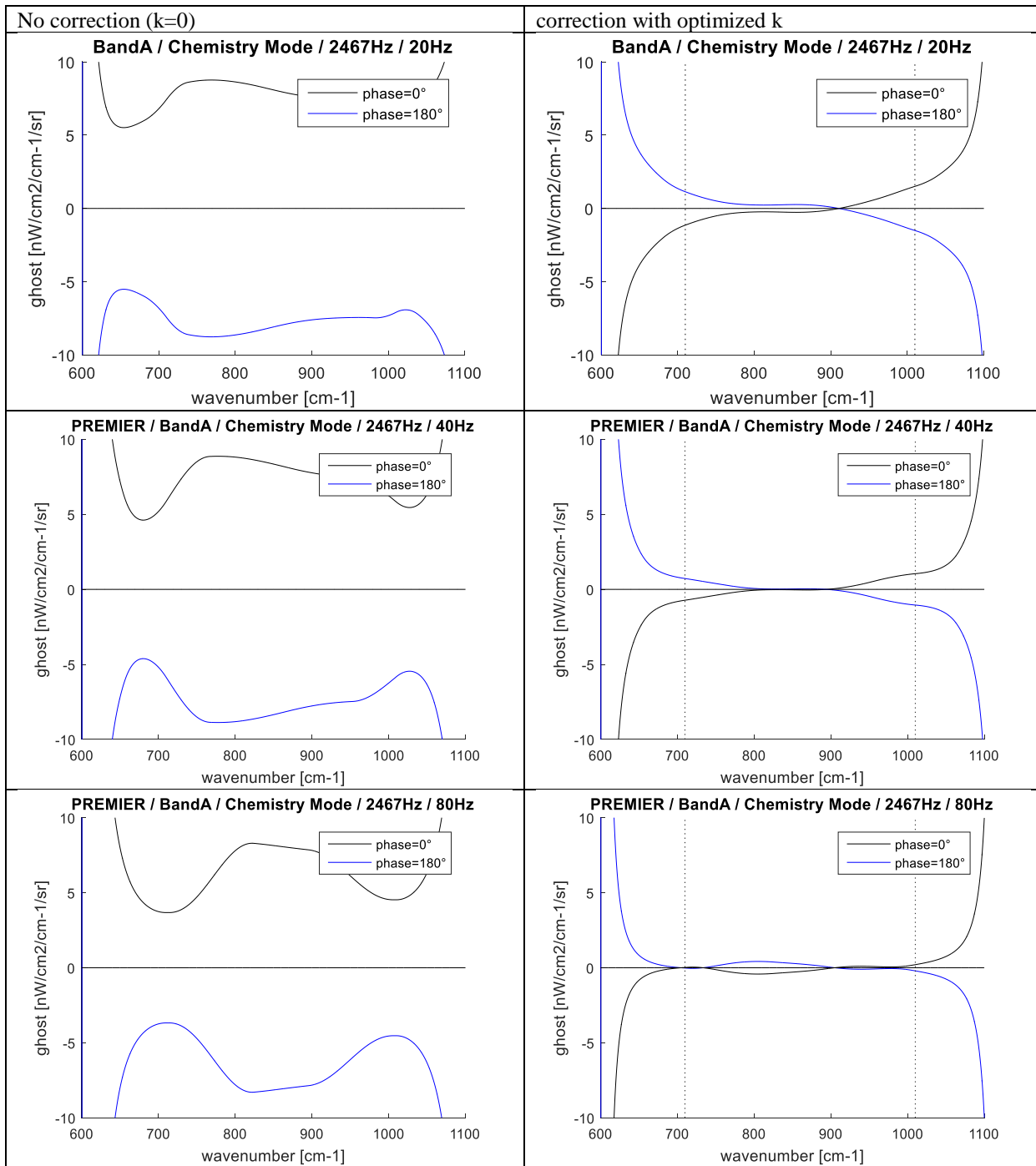


Fig. 5 The radiometric error for a broadband blackbody spectrum at 240K, in Premier's band A [710 cm^{-1} to 1010 cm^{-1}] in chemistry mode with detector sampling at 2467Hz. The panels give one disturbing frequency, from top to bottom, of 20, 40, 80Hz, respectively. The panels in the left column give the error without correction, while the right column shows the correction result.

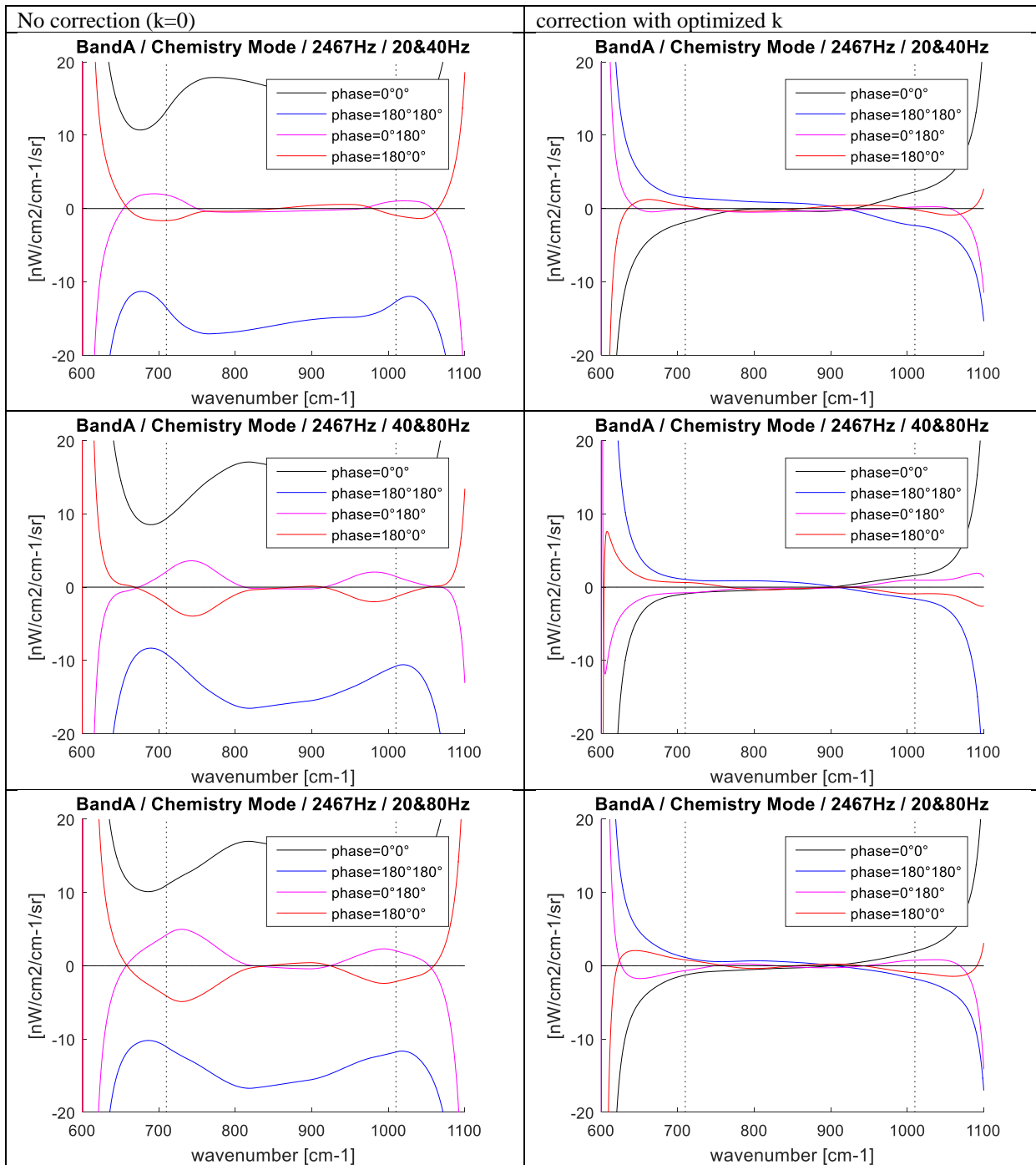


Fig. 6 The radiometric error for a broadband blackbody spectrum at 240K, in Premier's band A [710 cm^{-1} to 1010 cm^{-1}] in chemistry mode with detector sampling at 2467Hz. The panels give two disturbing frequencies, from top to bottom, of 20&40, 40&80, 20&80Hz, respectively. The panels in the left column give the error without correction, while the right column shows the correction result.

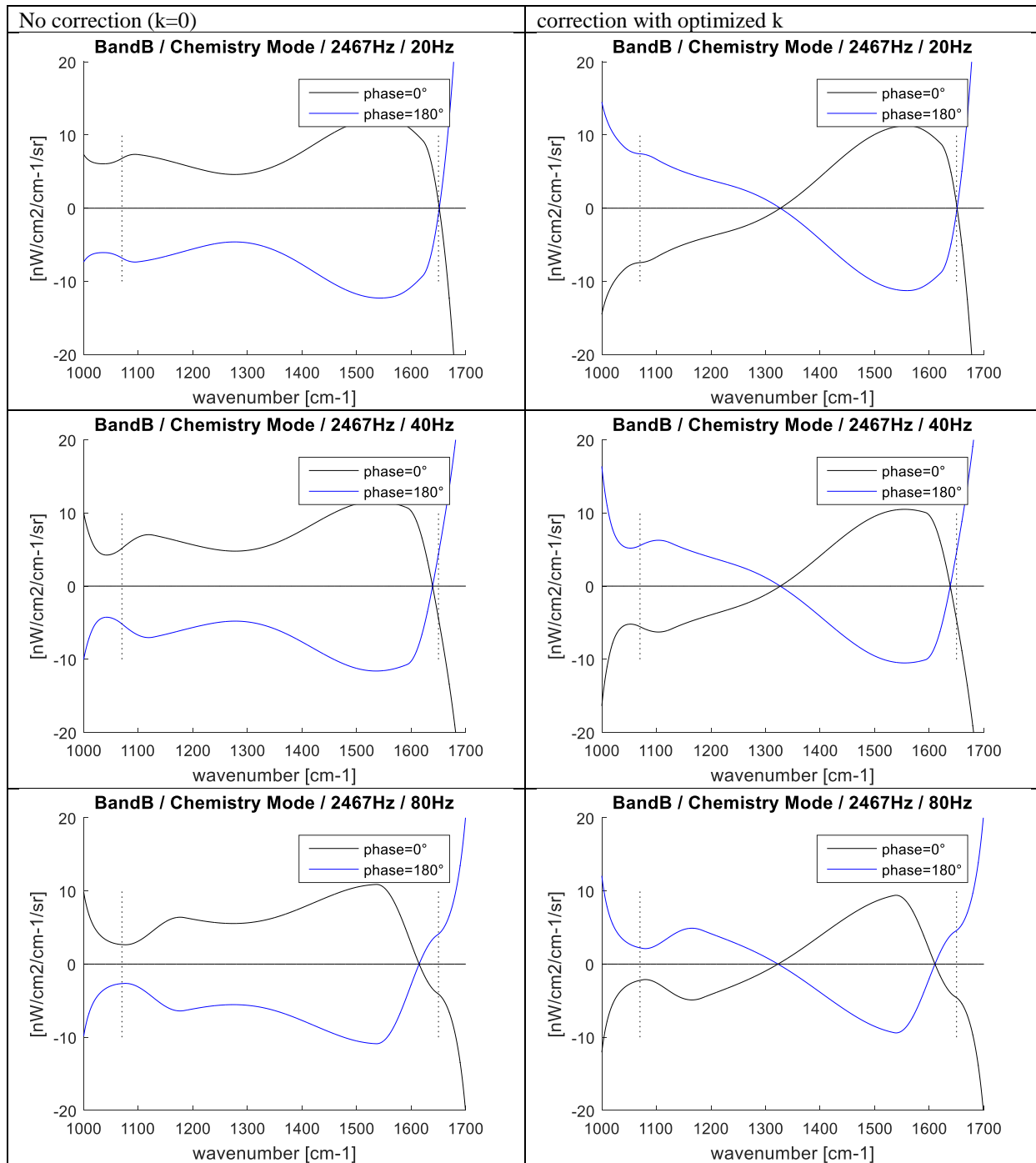


Fig. 7 The radiometric error for a broadband blackbody spectrum at 240K, in Premier's band B [1070 cm^{-1} to 1650 cm^{-1}] in chemistry mode with detector sampling at 2467Hz. The panels give one disturbing frequency, from top to bottom, of 20, 40, 80Hz, respectively. The panels in the left column give the error without correction, while the right column shows the correction result.

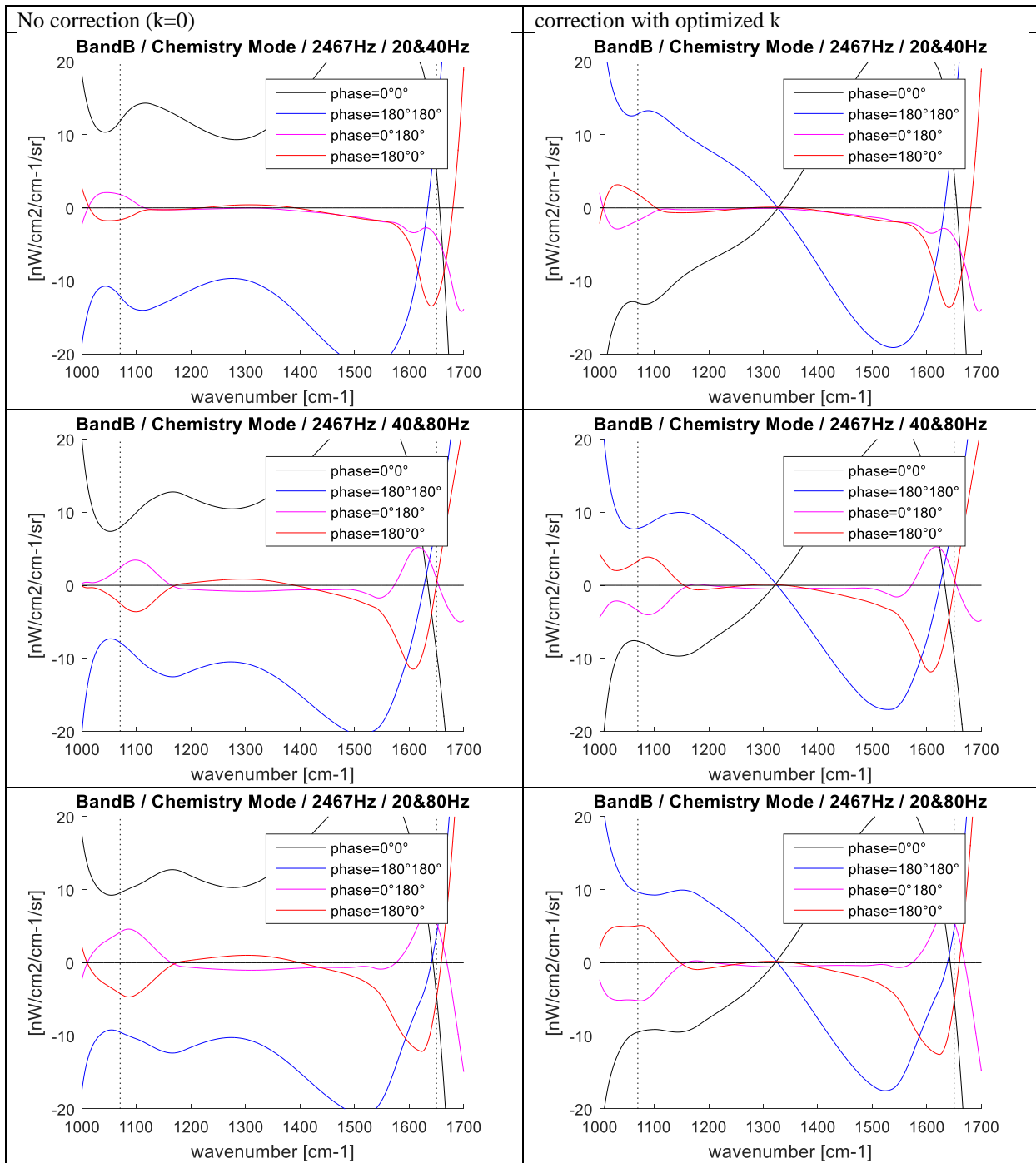


Fig. 8 The radiometric error for a broadband blackbody spectrum at 240K, in Premier's band B [1070 cm^{-1} to 1650 cm^{-1}] in chemistry mode with detector sampling at 2467Hz. The panels give two disturbing frequencies, from top to bottom, of 20&40, 40&80, 20&80Hz, respectively. The panels in the left column give the error without correction, while the right column shows the correction result.